BNL-49971

SOLAR NEUTRINO EXPERIMENTS: AN UPDATE

RICHARD L. HAHN
*Chemistry Department, Brookhaven National Laboratory **
Upton, New York 11973

ABSTRACT

The situation in solar neutrino physics has changed drastically in the past few years, so that now there are four neutrino experiments in operation, using dif ferent methods to look at different regions of the solarneutrino energysp ectrum. These experiments are the radiochemical ^{37}Cl Homestake detector, the realtime Kamiokande detector, and the different forms of radiochemical ^{71}Ga detectors used in the GALLEX and SAGE projects. It is noteworthy that all of these experiments report a deficit of observed neutrinos relative to the predictions of standard solar models (although in the case of the gallium detectors, the statistical errors are still relatively large). This paper reviews the basic principles of operation of these neu trino detectors, reports their latest results (as of July, 1993), and discusses some theoretical interpretations. The progress of three realtime neutrino detectors that are currently under construction, SuperKamiok ande, SNO and Borexino, is also discussed.

1. INTRODUCTION

Compared to the situation in solar neutrino physics several years ago, when there was only one operating solar neutrino experiment, namely the radiochemical ^{37}Cl detector operated by R. Davis and colleagues at the Homestake Mine [1], today the field is flourishing with three additional experiments providing data on solar neutrinos - Kamiokande [2], GALLEX [3], and SAGE [4] - and at least three more detectors under construction - Super-Kamiokande [5], SNO [6] and Borexino [7]. The great continuing interest in neutrino physics of course is due to the fact that, even with the new data from these solar neutrino experiments, the solar neutrino problem still persists: the different experiments, which are sensitive to different regions of the solar-neutrino energy-spectrum, all report deficits compared to the predictions of standard solar models. In this paper, I review the principles of operation of these different neutrino detectors, present their latest results (as of July, 1993), and discuss some of the theoretical interpretations that are currently in vogue. I also report progress in the construction and development of the new solar neutrino detectors.

2. BASIC OPERATION OF SOLAR NEUTRINO DETECTORS

Two broad categories of detectors are used in solar neutrino experiments: radiochemical detectors and on-line detectors. The characteristics of these two

different detector types are discussed in the sections below.

Because the cross-sections for neutrino interactions in matter are extremely small, all solar-neutrino detectors have certain features in common: They are very large, containing many tons of target material. They are situated in low-background environments, such as deep underground laboratories, so as to minimize cosmic-ray backgrounds. And strict controls of radioactive contaminants, especially of naturally occurring elements such as U, Th and Ra, are applied in selecting both the site of the laboratory and the construction materials for the detector.

2.1. Radiochemical Detectors

The operation of radiochemical detectors is governed by the principle that, as a result of an interaction with a neutrino, the target nucleus is transformed into a different nuclear species that can be chemically separated and removed from the bulk of target atoms with high specificity and efficiency. This method is employed to study the charged-current weak interaction, such as neutrino capture (also called inverse beta-decay), ${}^{A}Z + \nu_e \rightarrow {}^{A}(Z+1) + \beta^-$, where the product nucleus, because of its change in atomic number, has different chemistry from the target.

Often in neutrino capture, the product nucleus is radioactive, so that after it has been removed from the target and purified, its radioactive decay can be observed. *The combination of the measured energy spectrum and the half-life of the known product nuclide then serves as a characteristic signature for neutrino capture in the target.*

It has been suggested at times that other means of identification of the separated product nucleus be used, such as (accelerator-based) mass-spectrometry or resonance-ionization mass-spectrometry, particularly when the product is not radioactive. However, these alternate methods have not as yet been applied to an operating solar-neutrino detector.

Two types of thresholds determine the characteristics of a radiochemical neutrino detection system. The primary one is the Q-value of the chosen neutrino-capture reaction (equivalent of course to that of the inverse beta-decay process); as we shall see, often a very low threshold, well below 1 MeV, can be achieved. The second threshold is that of the counting system used to detect the radioactive decay of the product; this instrumental threshold can usually be set comfortably below the relevant decay energies, *e.g.*, $\approx$0.5 keV for gas-filled proportional counters.

During a "solar exposure" or "run" with a radiochemical detector, the target passively absorbs neutrinos, collecting the radioactive products during a period normally chosen to be about two half-lives. At the end of the exposure, the product is chemically extracted from the target, and a new exposure period begins. Because the radioactive product is detected off line, the target is a "black box", yielding no real-time information about the details of the neutrino interactions. Instead, the result of the experiment is a single number, namely the rate of formation of the product nuclei, the "production rate", given in Solar Neutrino Units, SNU

(1 SNU = 1 neutrino capture per second per 10^{36} target atoms). Offsetting these disadvantages are two very important factors: The first has already been mentioned, the very low neutrino-capture thresholds that are attainable. The second advantage is the extremely high selectivity of the method; typically, on the order of 10 product atoms can be removed from a target that contains $\approx 10^{30}$ atoms.

Thus, it is no accident that three of the four solar neutrino detectors that have obtained results to date are radiochemical, namely ^{37}Cl and ^{71}Ga (two detectors), with respective neutrino-capture Q-values of 0.814 and 0.233 MeV. It is also worth noting here that another radiochemical detector had been put into operation with the aim of searching for Tc produced by neutrino capture in Mo ores, but gave unreasonably high results that were attributed to contamination problems. [8]

2.2. On-line Detectors

As their name states, on-line detectors observe neutrino events as they occur in real time in the target. Many such schemes for experiments depend upon placing radiation detectors (counters, phototubes, etc.) either around or in the target material (usually a transparently clear liquid). Observations are then made of either (a) ν_e-capture, by detecting the resulting β particle and/or the radiation emitted from the excited product nucleus, or (b) neutrino elastic scattering, by detecting the resulting scattered electron. It is possible in principle to observe the neutral-current as well as the charged-current component in such neutrino interactions.

The major advantage of measuring on-line events is that detailed information about the interaction, such as the energy, direction and arrival time of the neutrino, can be obtained. However, there is an associated serious disadvantage of these detectors, namely that their operating thresholds are usually quite high, several MeV, so that, as we will see below, only a small fraction of the full energy-range of solar neutrinos is amenable to measurement. In addition, the ratio of the desired neutrino signal to other events in these detectors is usually very small. Typically, only about 1 in 10^4 original events survives the data cuts to be associated with an incoming neutrino.

Characteristic of the data obtained with on-line detectors are a neutrino angular distribution that is strongly peaked in the direction of the sun, a neutrino (or electron) energy-spectrum and a value of the neutrino flux integrated over energy. (Reminder: the unit of flux is particles cm^{-2} s^{-1}, not SNU.)

3. PREDICTIONS OF STANDARD SOLAR MODELS

The literature of nuclear fusion reactions in the sun, and of the concomitant production of neutrinos, is quite extensive. See for example Ref. 9 and also the talk by C. W. Kim at this workshop.

Relevant to the present discussion is the plot of the neutrino energy-spectra that is predicted by the standard solar model of Bahcall and co-workers [10,11].

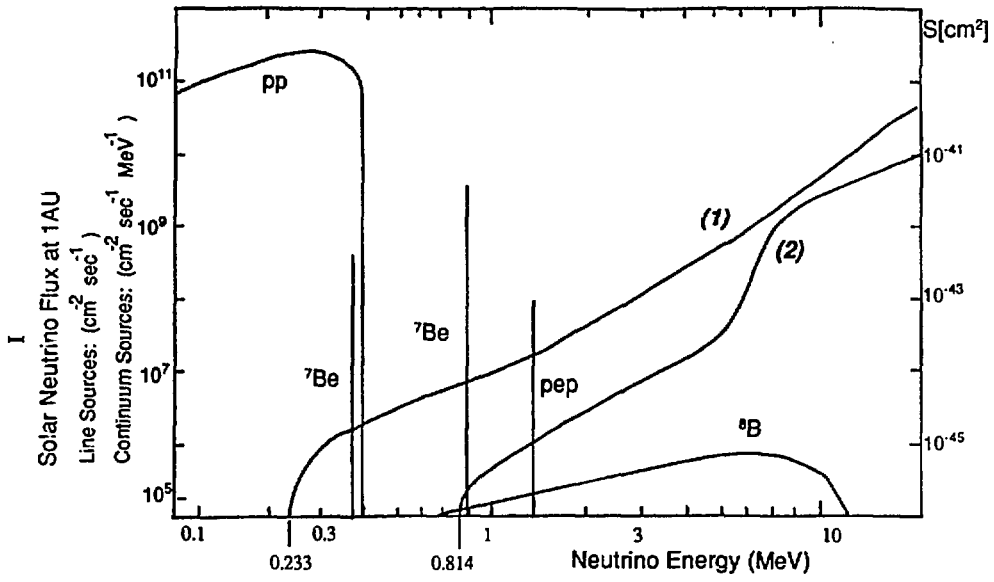

Fig. 1. Neutrino energy spectra for solar hydrogen burning [9]; flux units are given on left scale. Cross-sections (right scale) for ν_e capture are shown for ^{71}Ga (curve 1) and ^{37}Cl (curve 2).

Figure 1 shows the energy dependence of the fluxes expected at the earth from the solar "hydrogen burning" reactions that produce *pp*, ^{7}Be, and ^{8}B neutrinos. Not shown are the spectra expected from the solar CNO cycle. The figure also contains the response functions (excitation functions) for the ^{37}Cl and ^{71}Ga detectors, labelled (2) and (1) respectively, with cross-sections $\leq 10^{-40}$ cm^2.

The importance of the Q-values of the selected reactions is apparent in the figure. The ^{37}Cl detector, with its threshold of 0.814 MeV, is sensitive to the ^{7}Be and ^{8}B, but not to the *pp*, neutrinos. On the other hand, the ^{71}Ga detector, because of its threshold of 0.233 MeV, can see a major portion of the the main energy-producing reaction in the sun, the *pp* branch, as well as the higher-energy neutrinos. Detecting the *pp* neutrinos is especially important because their intensity is known from the measured solar luminosity. Note also that the lowest instrumental threshold attained by the Kamiokande on-line detector is 7.0 Mev, so that it is sensitive only to the upper portion of the ^{8}B spectrum.

The production rate of a radiochemical detector is the product of the flux and cross-section at each energy, integrated over energy, starting at the Q-value. Table 1 lists these rates in SNU for the ^{37}Cl and ^{71}Ga detectors, as predicted by two different solar models [11,13] for the different neutrino branches, including the ^{13}N and ^{15}O neutrinos from the CNO cycle. The predicted neutrino fluxes are also

Table 1. Predictions of two standard solar models.

ν_e-branch	ν_e Flux [a] ($cm^{-2}s^{-1}$)	^{37}Cl Rates[a] (SNU)	^{71}Ga Rates[a] (SNU)
pp	6.0 (6.0) $\times 10^{10}$	0.0 (0.0)	70.8 (70.6)
pep	1.4 (1.3) $\times 10^{8}$	0.2 (0.2)	3.1 (2.8)
^{7}Be	4.9 (4.2) $\times 10^{9}$	1.2 (1.0)	35.8 (30.6)
^{8}B	5.7 (3.8) $\times 10^{6}$	6.2 (4.1)	13.8 (9.3)
^{13}N	4.9 (6.3) $\times 10^{8}$	0.1 (0.1)	3.0 (3.9)
^{15}O	4.3 (5.6) $\times 10^{8}$	0.3 (0.4)	4.9 (6.5)
Sum		8.0 (5.8)	132 (124)

[a]Two numbers are listed for each entry: the first is from Ref. 11; the second, in parantheses, from Ref. 13.

listed, for comparison with data from on-line detectors.

4. EXPERIMENTAL DETAILS AND RESULTS

This section deals with each of the solar-neutrino detectors, points out significant experimental details, and summarizes the latest results, as of July, 1993. Much of this information and the figures that follow were provided to me by scientists working with the different detectors; they are acknowledged in section 7.

4.1. ^{37}Cl

The ^{37}Cl detector was developed by Davis and colleagues at Brookhaven National Laboratory [1]. The detector, which has been operating in the Homestake Mine (USA) since 1971, consists of 615 tons of the organic liquid, perchloroethylene, C_2Cl_4; the natural abundance of ^{37}Cl is 24.23%. The neutrino-capture reaction is $^{37}\mathrm{Cl} + \nu_e \rightarrow {}^{37}\mathrm{Ar} + \beta^-$, with a Q-value as previously noted of 0.814 MeV.

Because Ar is a noble gas, the chemical extraction of the radioactive ^{37}Ar from the target is effectuated in high yield by periodically bubbling helium gas through the liquid to sweep out the Ar atoms. After purification, the ^{37}Ar is added to P-10 counting gas, 90% Ar and 10% CH_4; this gas mixture is placed in a miniaturized proportional counter so as to optimize the counting efficiency. The signature of ^{37}Ar is the observation of the peak due to K x-ray and Auger-electron emission in electron capture, decaying with the characteristic 35.2-day half-life. The results from the ^{37}Cl detector [15] are shown in Fig. 2 for individual solar runs and for the

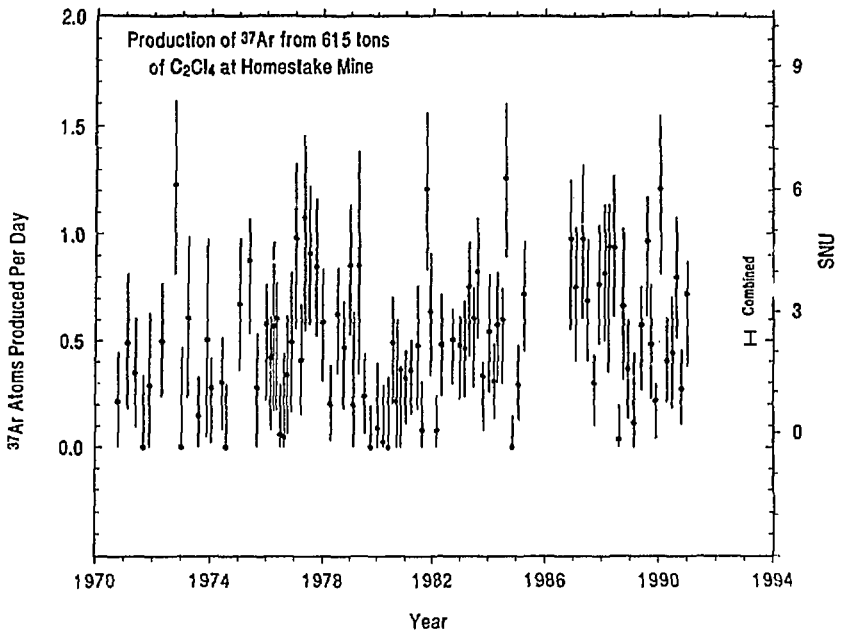

Fig. 2. Production rate of ^{37}Ar *vs.* time from the Homestake ^{37}Cl detector [15].

combined average value. It is impressive that this detector has been collecting data for more than 20 years.

From 1971-1990, 96 solar runs were done; 630 atoms of ^{37}Ar attributed to solar neutrinos were detected, equivalent to a mean production rate of 0.430 ± 0.043 atoms per day, or 2.28 ± 0.23 SNU [1,15]. In Table 1, values from two different solar models are listed for ^{37}Cl, 8.0 ± 1.0 SNU [11], and 5.8 ± 1.0 SNU [12,13]; both are in serious disagreement with the experimental value. This well-known discrepancy is called the "solar neutrino problem".

4.2. Kamiokande

Kamiokande, situated in the Kamioka mine (Japan), has been operating as an on-line neutrino detector since 1987 [2]. The target is purified light water (H_2O), with a total mass of 3000 tons; of this, 680 tons provide the fiducial volume of the target for solar neutrino detection, with the remaining mass of water serving as shielding around the target. Neutrinos are detected as a result of their elastic scattering from electrons in the target medium; the forward-scattered electrons emit Cerenkov radiation that is recorded in the multiple phototubes that view the target. The trajectories of these electrons, and therefore of the incoming neutrinos, are then reconstructed from these signals. Kamiokande has gone through several modifications to improve its operation and to reduce backgrounds, such as the installation of chemical purification equipment to remove naturally occurring radioactive contaminants, such as Rn, from the water. As these improvements have occurred, the

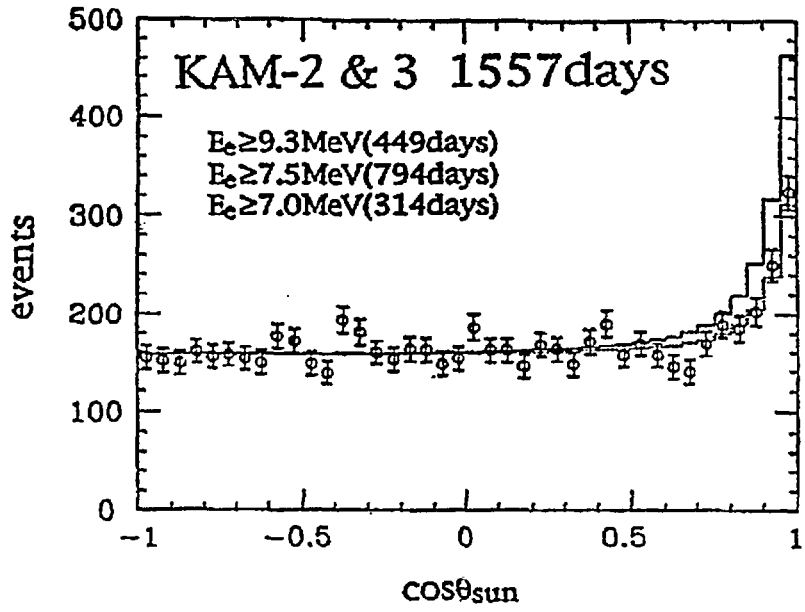

Fig. 3. Angular distribution of neutrino events relative to the sun's direction recorded by Kamiokande-2 and -3 [5].

threshold for neutrino detection has dropped. In Kamiokande-2, the threshold was 9.3 MeV; in the improved Kamiokande-3, it was lowered to 7.5 and then to 7.0 MeV [16]. As noted earlier, in all of these stages, Kamiokande has been sensitive only to ^{8}B neutrinos.

Figure 3 shows the composite results from Kamiokande-2 and 3, obtained during 4.27 years of data-taking [5]. These data, which have survived the various cuts that remove non-neutrino-related events, are plotted *vs.* the cosine of the angle between the detector and the sun (the position of the sun in the sky is known from the recorded time of each event). The data (dotted curve) are seen to peak at $\Theta_{sun} = 0$, whereas the rest of the measured angular distribution is essentially flat. There are 493 observed events in the peak. The solid curve in the figure is that predicted by the standard solar model. In Fig. 3, the ratio of measured to predicted events is equal to 0.50 ± 0.04 (stat.) ± 0.06 (syst.) relative to the value of the ^{8}B flux calculated in the solar model of Bahcall and Ulrich [11]; if the comparison is instead made with the solar model of Turck-Chieze and Lopes [13], the flux ratio is 0.66 ± 0.06 ± 0.08. In either case, a substantial fraction of the predicted neutrino flux is missing. Qualitatively speaking, these Kamiokande results confirm the solar neutrino deficit first recorded by the ^{37}Cl experiment (neglecting details such as the different energy thresholds of these two neutrino detectors).

It is interesting to note that in Ref. 2 the Kamiokande collaboration extracted a ^{8}B neutrino energy-spectrum from their data. Such information has relevance to neutrino-oscillation mechanisms. In their more recent reports, they have

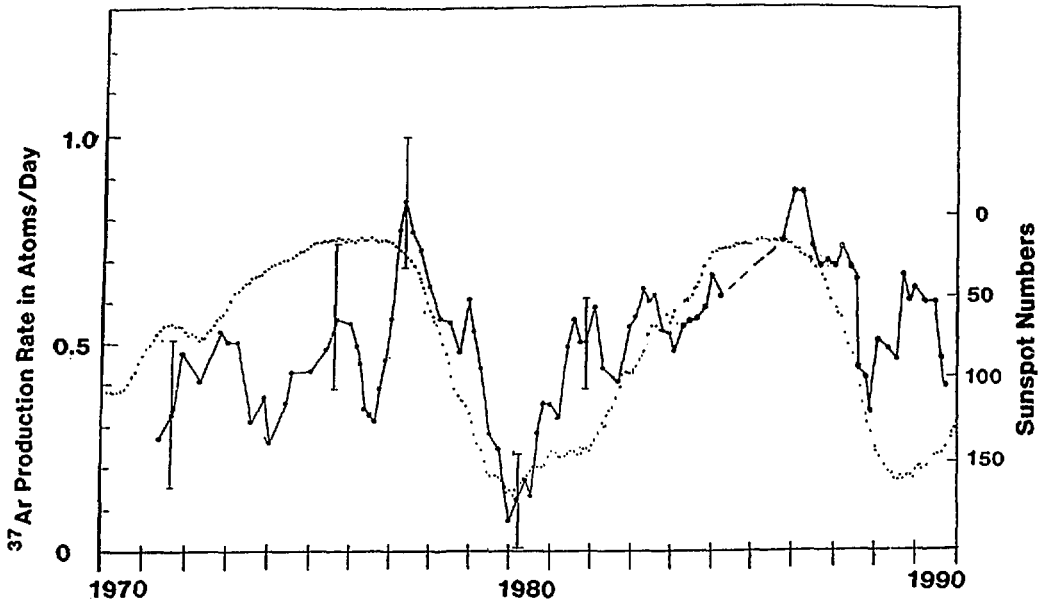

Fig. 4. Comparison [14] of the variation over time of the production rate of ^{37}Ar from the ^{37}Cl detector (points and solid curve) with the inverse of the number of sunspots (dotted curve). The data points are "running five-point averages"; see text.

not as yet shown an updated energy spectrum with improved counting statistics.

4.3. Temporal Variations of Solar Neutrinos?

Davis has pointed out that data taken with the ^{37}Cl detector over two decades seem to show an anti-correlation with sunspot activity [14]. Figure 4 shows his radiochemical data points, plotted as a "running five-point average" (left scale) *vs.* time; in this method of averaging, the results of the first five runs taken in time sequence from Fig. 2 are averaged, the first run is then discarded and the sixth run in the sequence is added to the group, and a new average is calculated, *etc.* Davis has claimed that the inverted plot of sunspot activity, the dotted curve in Fig. 4 (right scale), and the averaged neutrino points qualitatively show the same variation with time.

This purported connection of solar neutrino production (for ^{7}Be and ^{8}B neutrinos) and sunspot activity has engendered much discussion in the literature, because no obvious mechanism exists to couple the two phenomena: *i.e.*, solar neutrinos are produced in the solar core while sunspot activity is a magnetic phenomenon near the solar surface. Some authors have avoided the dilemma by claiming that the measured solar neutrino variation shown in the figure is not statistically significant, while others have chosen to accept the premise that such an effect exists and to explore its significance. The interest in this regard is mainly from a theoret-

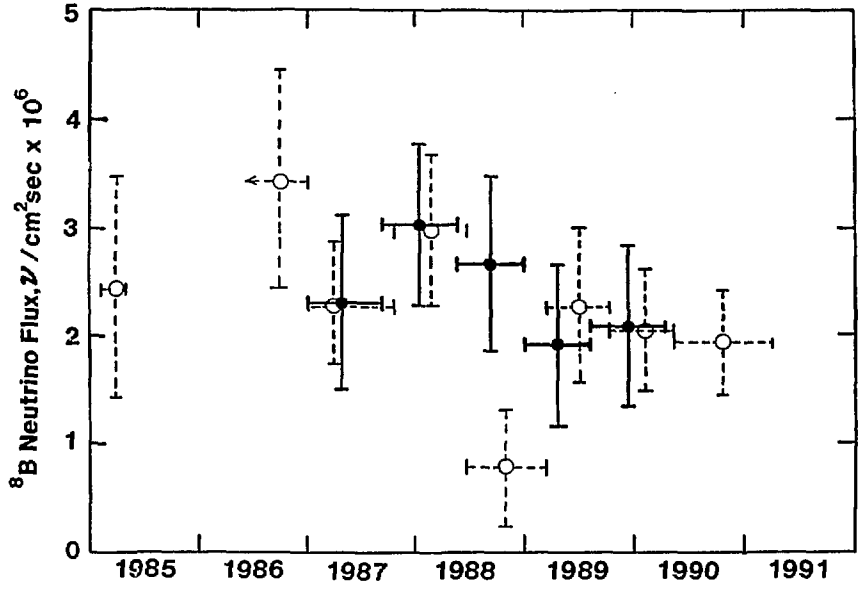

Fig. 5. Comparison of the variation over time of the flux of ^{8}B neutrinos, as derived from the ^{37}Cl data (open points) [15] and as reported by Kamiokande (closed points) [5]. See text.

ical viewpoint; mechanisms have been conceived of that involve neutrino magnetic interactions, the possibility of a non-zero neutrino-magnetic-moment, *etc.*

An experimental test of this possible correlation of neutrino flux and sunspot activity was done by the Kamiokande group by searching its data for neutrino-flux variations that occurred during the period 1987-1992 [5]. It concluded unequivocally that there was no detectable variation of the solar neutrino flux, as shown by the closed points in Fig. 5, thus *refuting* the claim from ^{37}Cl of a correlation with sunspot activity.

This subject becomes even more intriguing as a result of a recent analysis by Davis [15]. He calculated the average values of his ^{37}Ar production rates for time bins that he selected to be identical to those used in the Kamiokande analysis. He then converted these rates into ^{8}B neutrino fluxes by taking account of the predicted fraction of his signal that is due to ^{8}B neutrinos (see Table 1). The results of his analysis are shown in Fig. 5, where his derived ^{8}B flux values are plotted as open points, and the five Kamiokande values, as closed points; two additional Kamiokande points for 1991 and 1992, not shown in the figure, are very similar in value to the points that are shown. Davis concludes that, except for his low point in 1988, his values *agree* point by point with the Kamiokande values. He also notes that, for the period January 1987 to May 1991, the two experiments agree on the average values of the ^{8}B flux: 2.04 ± 0.31 from ^{37}Ar, 2.39 ± 0.35 from Kamiokande

(in units of 10^6 cm^{-2} s^{-1}).

What are we to make of this comparison? The point of Davis' analysis is that the time bins used by Kamiokande are too coarse to reveal any temporal variation; his data, when treated in the same way, do not show much variation either. One other result of his analysis: for this four-year period that overlaps the Kamiokande data, eighteen ^{37}Cl solar runs gave a mean total production rate (*i.e.*, for all neutrino branches above the 0.814-MeV threshold) of 2.86 ± 0.40 SNU, which is higher than his twenty-year mean of 2.28 ± 0.23 SNU quoted earlier. Davis infers that this increase is statistically significant and is further evidence for a solar neutrino output that changes over time. On the other hand, he does point out that his recent data, plotted in Fig. 2 for the period beginning in 1989, do not exhibit the expected correlation with solar activity, *i.e.*, the measured neutrino rates did not continue to decrease as the sunspot number increased during that period. No explanation has been offered for this change in the trend of his data.

I leave it to the reader to interpret these different, sometimes conflicting, arguments. The possibility of temporal variations in solar neutrino production is still an open question.

4.4. ^{71}Ga: GALLEX and SAGE

4.4.1. Operation of the Two Detectors

There are two operating radiochemical detectors that use ^{71}Ga (natural abundance, 39.89%) as the target in the reaction $^{71}\text{Ga} + \nu_e \rightarrow {}^{71}\text{Ge} + \beta^-$: SAGE and GALLEX (I am a member of the GALLEX collaboration). SAGE is located in the Baksan Neutrino Observatory (Russia); GALLEX, in the Gran Sasso National Laboratory (Italy). This situation of two radiochemical detectors that use the same neutrino reaction is quite unusual because such neutrino-detection experiments not only are very expensive, but also require many years of intensive effort before any reliable data are forthcoming. Yet, having two very similar, if not identical, detectors offers the unique possibility of independent verification of a solar neutrino measurement.

The basic operation of the gallium detector is analogous in many ways to that of the ^{37}Cl detector. This situation is understandable when it is realized that much of the early research, especially of the chemistry, of the ^{71}Ga detector was done at Brookhaven. However, the product of the neutrino capture, ^{71}Ge, is not a noble gas as is ^{37}Ar, so some ingenuity had to be used to find successful chemical procedures, to separate Ge from the target, and to prepare a Ge compound that is suitable for low-level counting. The key to the removal of the radioactive ^{71}Ge product from the Ga target is the formation of a volatile compound, $GeCl_4$, which can be entrained in a stream of gas. The extraction of this compound is quantitative, ≈100%. This product is then converted to another gaseous compound, GeH_4, which is a suitable counter-filling gas; this compound is purified by gas chromatography, mixed with Xe and put into a (miniaturized) proportional counter. Xe is added to the counter

to increase the counting efficiency for the energetic x-rays emitted in the decay of ^{71}Ge. The signature of ^{71}Ge is the observation of the K and L peaks from electron capture, decaying with the characteristic 11.43-day half-life.

The chemical forms of the gallium targets used in GALLEX and SAGE are different, and so their initial chemical procedures also differ. The GALLEX target contains 30 tons of gallium in a concentrated aqueous solution of $GaCl_3$ (8 M) and HCl (2 M). Under these conditions, any Ge, such as that formed by ν_e capture, will automatically tend to form volatile $GeCl_4$. This product is then extracted by bubbling an inert gas, N_2, through the liquid target. SAGE uses liquid Ga metal (melting point, 29.8 °C) as its target; the experiment began with 30 tons of metal, which was increased to 57 tons in mid 1991. To remove any Ge formed in the target, an aqueous mixture of HCl and the oxidant, H_2O_2, must be vigorously mixed with the molten Ga metal. $GeCl_4$ is formed and migrates to the aqueous phase, from which it can then be removed in the usual manner, in a gas stream. From this stage on, the chemical and most of the ensuing steps used by SAGE and by GALLEX are very similar.

One difference to be noted between SAGE and GALLEX is in the ^{71}Ge energy-spectra obtained with their low-level counting systems. Since their solar data-taking began, GALLEX has had the capability of detecting both the L (1.17 keV) and K (10.37 keV) peaks, while SAGE until very recently has been able to count only the K peak, because of excessive background and/or noise in the L-region of their spectrum.

In the start-up phases of both experiments, even though great care was taken to avoid radioactive contaminants, similar problems were encountered. The first, which was initially rather serious, was due to the fact that several radioactive germanium isotopes are produced by cosmic-ray bombardment while the gallium target material is above ground, before being brought into the underground laboratory. One isotope, ^{68}Ge, has a very long half-life, 271 days, and a decay mode that is very similar to that of ^{71}Ge. It was found that an extremely small but non-negligible fraction of this cosmogenic ^{68}Ge unaccountably remained in the gallium target. Although it was removed only slowly by the usual chemical steps, the number of extracted ^{68}Ge atoms was high enough to raise the counter backgrounds to a level where it was not possible to see the decay of the $\approx$1 atom per day of ^{71}Ge expected. Special steps had to be taken, such as heating the 101 tons of GALLEX target solution or cleaning anew the SAGE target containers, to reduce the ^{68}Ge to acceptable levels; these steps were done successfully. However, the start-up of both SAGE and GALLEX was delayed by several months before their "^{68}Ge problems" were solved.

A second problem, common to both experiments, was due to the fact that ^{222}Rn is an environmental contaminant. For example, the radioactive non-volatile daughters of Rn can deposit on the outside of the counters and contribute to the background. In addition, GALLEX found that a few atoms of ^{222}Rn somehow manage to find their way into the counters, even though the gas chromatography does separate Rn from GeH_4 with high efficiency. Since some Rn decay events fall

in the energy regions of interest for ^{71}Ge, it is of vital importance that Rn events not be mistaken for those from ^{71}Ge. In GALLEX, we have learned to identify Rn counts definitively; typically, we find ≈3 atoms of Rn in a counter, which on average produce 1 distinctive count that can be vetoed.

4.4.2. Results from the Two Gallium Detectors

The story of the comparison of SAGE and GALLEX results is complicated. I think it is clearest if told in a chronological way.

Of the two detectors, SAGE was the first to begin taking solar data. The first results came from five runs, which were presented at a conference in mid 1990 and then published in late 1991 [4]. These results contained no clear evidence for ^{71}Ge, and therefore, no evidence for solar neutrinos entering the target. The best fit to the data gave a production rate of 20 ± 17 (stat.) ± 32 (syst.) SNU; a more conservative analysis set an upper limit, <55 SNU at the 68% confidence level. These values are to be compared with solar model predictions (Table 1) of 132 SNU [11], and 124 SNU [13].

GALLEX presented its first results from 14 runs at the 1992 Granada conference and also in two concurrent publications [3,17]; note that some of the SNU values were called "preliminary" because counter backgrounds for those runs were still being measured. The characteristic energy spectrum and decay curve of ^{71}Ge were measured, showing clear evidence of a solar neutrino signal. The measured production rate was 83 ± 19 ± 8 SNU, which was (67 ± 16)% of the standard model prediction [11]. Significantly, GALLEX claimed that this relatively large measured production rate provided the first direct evidence for solar *pp* neutrinos.

Later, at the 1992 Dallas conference [18], SAGE presented new data from seven additional runs, done through 1991, which did contain evidence for a solar neutrino signal. Their new production rates were similar to the GALLEX values. Taking the data from all 12 of their runs, SAGE reported a combined mean value of 58 ± 21 ± 14 SNU, 44% of the model prediction.

Finally, at the present time, July, 1993, GALLEX in a new publication [19] has reported its final data from the 14 earlier runs plus data from seven additional runs. Its new mean rate for ^{71}Ge, obtained from 98 *K* and *L* events observed in 21 runs, is 87 ± 14 ± 7 SNU. To date, SAGE has not updated its 1992 reported value, which corresponds to 24 *K* events. I have been told that new SAGE data are being analyzed and will be presented later this year.

Figs. 6 and 7 present the most recent GALLEX results [19]. Fig. 6 presents the decay curve of the combined data from the 15 runs that have been completed; the solid line is a maximum-likelihood (M-L) analysis of the data, done with 11.43-day ^{71}Ge, a small contribution from 271-day ^{68}Ge, and a constant background. The χ^2 fit to the data, taking the theoretical values from the M-L curve, is seen to be quite acceptable for 20 degrees of freedom (22 time bins). Fig. 7 shows the results of the 21 individual GALLEX runs, analogous to Fig. 2 for ^{37}Cl.

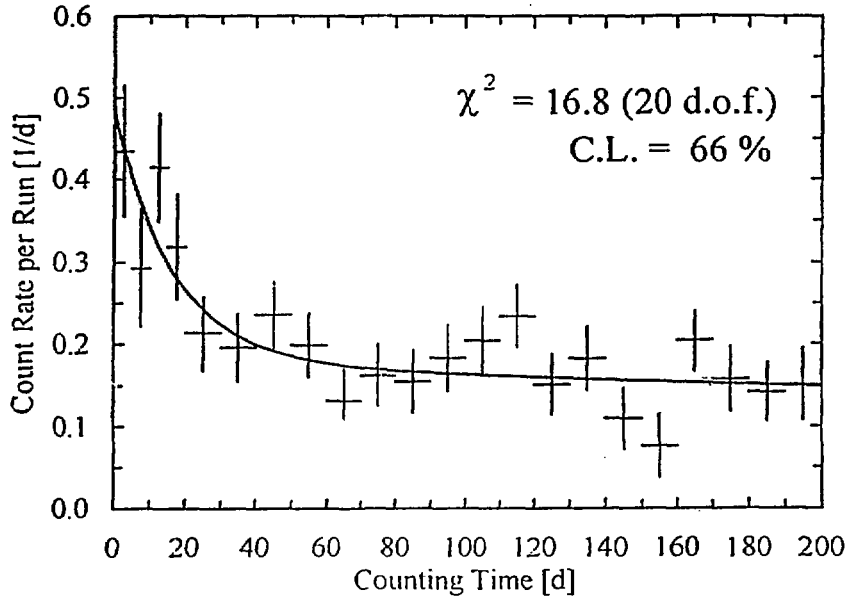

Fig. 6. Decay data from the 15 GALLEX runs that have been completed [19]. The points are the average count rates per run, for counting-time bins shown by the horizontal bars. The solid curve is the maximum-likelihood solution for 11.43-day ^{71}Ge plus 2 longer components, as described in the text.

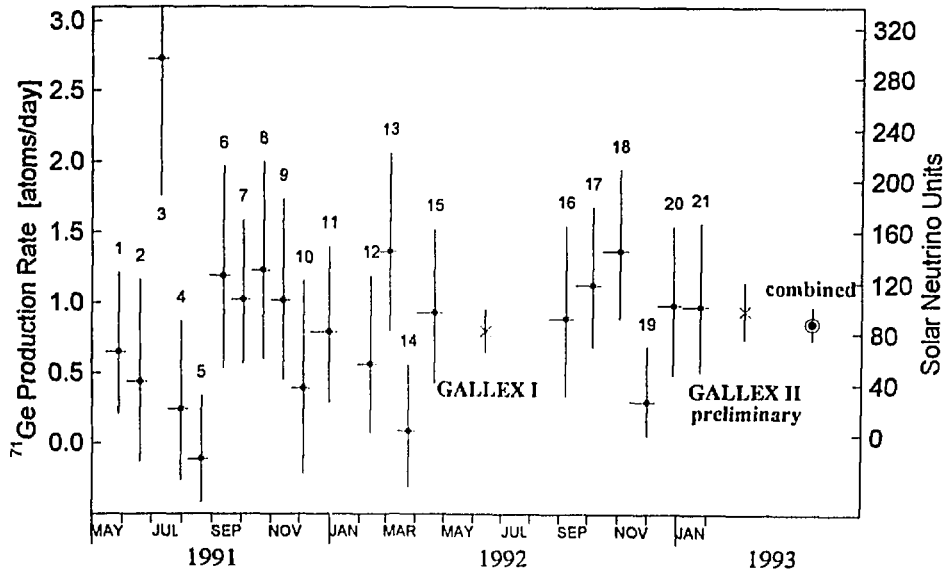

Fig. 7. Variation with time of the production rate of ^{71}Ge from the 21 GALLEX runs [19]. The right scale is the production rate in SNU from solar neutrinos, while the left scale is the total rate from all known sources (solar plus "side reactions").

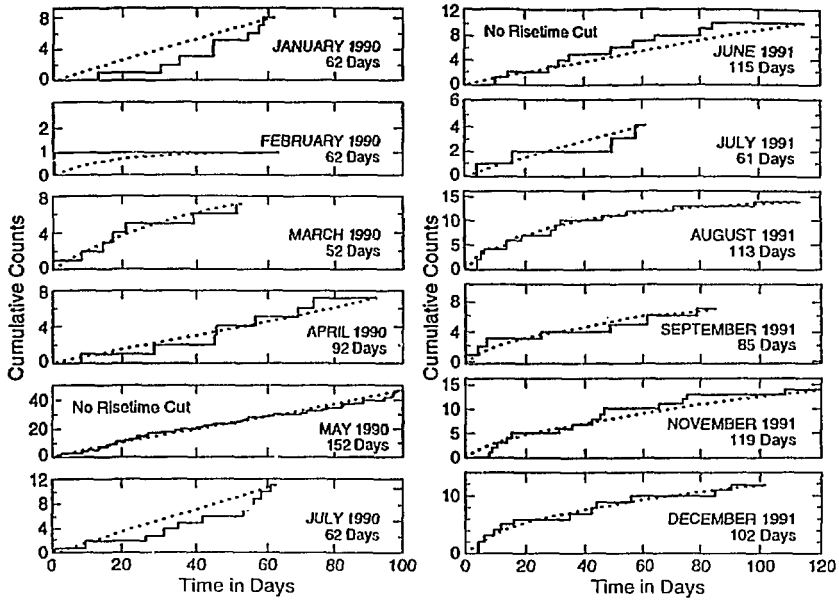

Fig. 8. Counting results from individual SAGE runs, shown as accumulated counts *vs.* time. Data are the solid histograms; maximum-likelihood fits are the dashed curves [18].

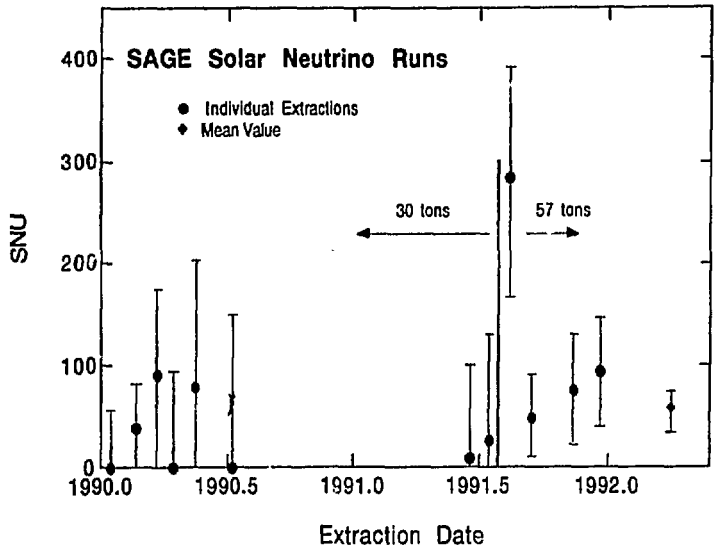

Fig. 9. Variation with time of the production rate of ^{71}Ge in SNU from SAGE [18]. Note the increase in target mass in 1991.

Fig. 8 shows the decay data from the 12 individual SAGE runs [18]. The results are shown as counts accumulated during the counting period ("integral counts"): the solid histograms are the data and the dashed curves are the maximum-likelihood fits. Note that a constant count rate, such as a background, will give a straight line in this plot, while a decaying component will have curvature. The dates of the runs and the length of each counting cycle are shown. The corresponding production rates of ^{71}Ge from these 12 SAGE runs are shown in Fig. 9.

Both GALLEX and SAGE continue to do solar runs, so their statistical errors and possibly the systematic errors as well, should decrease as more data are accumulated and improvements are made in the experiments. One item of note is that both groups are planning to do independent, full-scale, comprehensive tests of their experiments by "replacing" the solar neutrino signal with a more intense signal from a radioactive source. The isotope chosen as the source is 28-day ^{51}Cr, which decays by electron capture, emitting neutrinos. It is produced in a nuclear reactor, by irradiating kilograms of enriched ^{50}Cr with a high flux of thermal neutrons. The decay rate of the source, and therefore its rate of neutrino emission, can be determined directly, *e.g.* by measuring the intensity of its 310-keV γ ray. Irradiating the gallium target with this known source and measuring the number of ^{71}Ge atoms extracted will show if all facets of the experiment are working properly. Both GALLEX and SAGE plan to do these tests with ^{51}Cr sources of $\approx$37 PBq (1MCi) intensity in mid 1994.

5. INTERPRETATION OF THE DATA

Discussions of the standard solar models and of explanations of the solar neutrino problem in terms of neutrino oscillations have been discussed by many others, including C. W. Kim at this workshop. Although the scope of my talk is experimental, I will make a few comments about interpretations of existing solar neutrino data.

As noted above, all four neutrino experiments to date have reported deficits. The latest experimental values (reported above) divided by the theoretical predictions [11] are: 0.29 $\pm$ 0.03 for ^{37}Cl, 0.50 $\pm$ 0.07 for Kamiokande, 0.66 $\pm$ 0.12 for GALLEX, and 0.44 $\pm$ 0.19 for SAGE. In this comparison, the statistical errors in the theoretical values have been neglected and the statistical and systematic errors in the measurements have been combined in quadrature.

In its paper on the implications of these results [17], the GALLEX collaboration stated that the gallium result, taken by itself with its present large statistical error, was not in violent disagreement with the solar model predictions. However, they concluded that it was extremely difficult (but not impossible) to alter the standard solar models enough to have them agree with the results of all of the solar neutrino experiments. For example, trying to fit the experimental data by simply varying one theoretical parameter, the temperature of the solar core, while taking

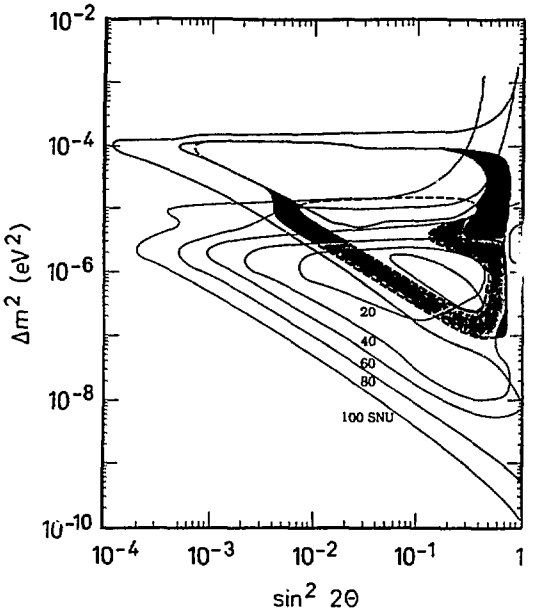

Fig. 10. MSW plot as presented by GALLEX in Ref. 17. The contour plots were calculated for the ^{71}Ga detector. The gray regions are consistent with the results from ^{37}Cl and Kamiokande, while the smaller black regions also include the GALLEX results. See text.

into account the predicted exponential temperature dependences of each neutrino branch [9], *pp*, ^{7}Be and ^{8}B, led to a temperature change in the core that was so large that it was unphysical.

On the other hand, GALLEX concluded that neutrino oscillations in matter, as described by the MSW effect [20], could satisfactorily explain the existing solar neutrino data. Figure 10 shows the MSW plot taken from Ref. 17 with calculated contours drawn for ^{71}Ga. The gray regions are consistent with the results from ^{37}Cl and Kamiokande, while the black regions also include the GALLEX results. We see that the results from the three different detectors narrow the available combinations of Δm^2 and the mixing angle, Θ, to two to three limited regions in the MSW plot (where $\Delta m^2 = m_1^2 - m_2^2$, and m_i is the mass of the ith mass-eigenstate). The Δm^2 values fall in the range, 10^{-5} - 10^{-6} eV^2. Thus, if $m_2 \gg m_1$, m_2 is on the order of meV, much smaller than the upper limits of several eV derived from β-decay end-point experiments (as discussed by R. G. H. Robertson at this workshop).

A much more detailed examination of these ideas was presented recently by Bludman *et al.* [21], who also considered the theoretical dependence of neutrino fluxes on core temperature. Because they could not obtain a consistent fit to all of the neutrino data, they concluded that no astrophysical explanation of the solar neutrino problem was possible. Bludman *et al.* also did a series of MSW calculations, and noted that their results for the combined data from the four detectors were

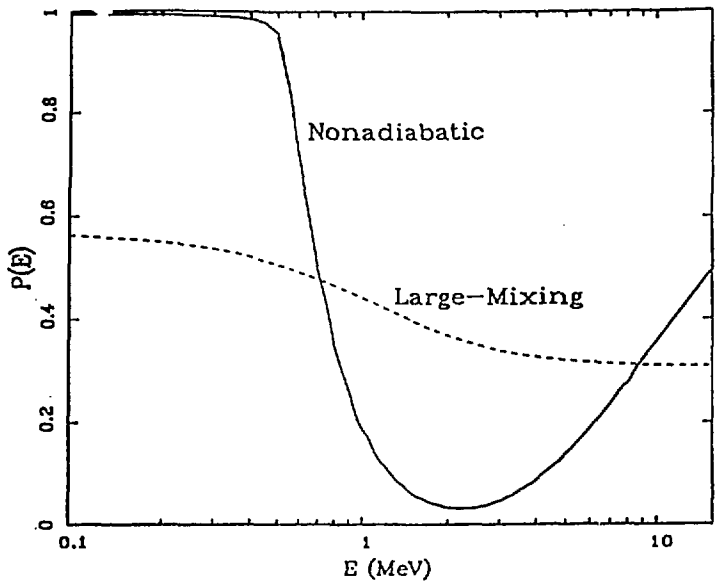

Fig. 11. Plots of the survival probability for solar neutrinos, *P(E)*, *vs.* neutrino energy [21]. MSW fits to the experimental data, analogous to what is shown in Fig. 10, were done, resulting in unique parameter sets for the nonadiabatic and large-mixing-angle solutions; see text for the values. These parameters were then used to calculate the *P(E)* curves.

indistinguishable from the GALLEX MSW plot shown in Fig. 10. These authors went further in their treatment of the MSW theory and used the data to obtain a unique fitted set of the theoretical parameters, Δm^2 and $\sin^2 2\Theta$: their respective values are 4.9×10^{-6} eV^2 and 8.3×10^{-3} for the nonadiabatic MSW solution, and 9.8×10^{-6} eV^2 and 0.76 for the large-mixing-angle MSW solution. For each set of these parameters, they then calculated values of *P(E)*, the probability of survival of ν_e in the sun as a function of neutrino energy. Their *P(E)* curves are shown in Fig. 11.

It is interesting to note in Fig. 11 that below 0.42 MeV, the maximum energy of *pp* neutrinos, the value of *P(E)* is appreciable for each MSW solution, especially for the nonadiabatic case where $P(E) \approx 1$. This prediction, that the majority of *pp* neutrinos survives the matter oscillations, supports the GALLEX claim for the observation of *pp* neutrinos.

We also see in Fig. 11 that the nonadiabatic solution reduces the flux of ^{7}Be neutrinos most severely (especially for the major component at 0.86 MeV) and the ^{8}B neutrinos to a lesser extent. Contrastingly, the large mixing-angle solution has a less pronounced energy dependence that affects all of the neutrino groups similarly.

These comparisons of the results of the four solar neutrino experiments with both the standard solar theory and the MSW theory suggest that neutrino matter-

oscillations are possible, although reduction of the statistical errors in the ^{71}Ge results is needed to tighten the constraints on the standard solar model (another possibility is vacuum oscillations [22]). However, all of the experiments have only noted the disappearance of ν_e. None has provided direct evidence for oscillations, the so-called "smoking gun", such as (a) the observation of the other neutrino flavors, ν_μ or ν_τ, to make up the neutrino deficit, or (b) the distortion of the ν_e energy-spectrum. Such data will have to await the completion of the new generation of on-line solar neutrino detectors, some of which I discuss below.

6. NEW DETECTORS

In this section, I will briefly discuss three on-line detectors that are in various stages of construction and are expected (or hoped) to become operational in the near future, in the period 1995-97: Super-Kamiokande, SNO and Borexino. One goal of all of these detectors is to achieve much higher data collection rates than the neutrino detectors that are operating today. There are many other concepts that have been proposed as solar neutrino detectors, which are in various stages of development, but will most likely not come on line in the near future; none of these will be reviewed here.

In principle, all of these detectors will be able to measure the energy spectrum of the solar neutrinos. This characteristic is important because observation of shifts or distortions in the neutrino energy-spectrum should be one of the signatures of neutrino oscillations, since the neutrino-oscillation probability, *P(E)*, has a sensitive energy dependence. Such spectral distortions are not expected to occur if the observed deficit of ν_e is due to astrophysical causes.

6.1. Super-Kamiokande

A major expansion at the Kamioka site (Japan), Super-Kamiokande, is being undertaken at present [5]. Its principles of operation, based on detection of neutrino-electron elastic scattering, are identical to those of Kamiokande. However, major improvements are being implemented. For example, the new detector will contain 50000 tons of purified H_2O; the fiducial volume containing 22000 tons of H_2O will be viewed by 11200 large photomultiplier tubes. Improved electronics and purification processes to remove radon and other naturally occurring radioactive impurities will be installed.

Super-Kamiokande is scheduled to begin taking data in 1996. Its goal is to achieve significant improvements relative to Kamiokande: to reduce the detection threshold from 7 to 5 MeV and to accumulate about 100× as much data.

Super-Kamiokande will not be able to distinguish the neutral-current from the charged-current signal. But its high data rate and low threshold should allow it to recognize distortions in the electron-energy spectrum that should result from neutrino oscillations. It should also see an appreciable day-night effect (*i.e.*, additional oscillations occurring for those neutrinos that pass through the Earth on the

way to the detector) in the large mixing-angle region that is allowed in the MSW plot, as shown in Fig. 10.

6.2. SNO

SNO is an acronym for the Sudbury Neutrino Observatory [6]. It is currently being constructed in the Sudbury mine (Canada) at the 6800-feet level (2073 m), where the excavation of the cavity that will house the detector was completed in April 1993.

The target in SNO is 1000 tons of heavy water, D_2O, placed in a thin-walled transparent vessel that will float in an outer container filled with H_2O. Some 9500 large photomultiplier tubes placed in the H_2O vessel will surround the D_2O to observe the Cerenkov radiation resulting from neutrino-induced reactions in this medium. The completion of the SNO construction is scheduled for April 1995; filling of the detector vessel with the water and the start of data acquisition should occur in September 1995.

Several different neutrino reactions give this detector great versatility. As in Kamiokande, neutrino-electron elastic scattering will be detected to determine the trajectories of the incoming neutrinos ("directionality to the neutrino source"). This detection mode will also provide some sensitivity to different electron energies. As in Kamiokande, the major contributor to the elastic scattering signal will be ν_e, for the scattering cross-section for the neutral-current interaction is $\approx 1/6$ that of the charged-current.

Those reactions that occur between neutrinos and the deuterium in the target give SNO its unique characteristics. The ν_e-capture reaction (which is observed by the radiochemical detectors) can also be detected in SNO, on-line, via the Cerenkov light from the electrons emitted in the reaction, $^2D + \nu_e \rightarrow p + p + \beta^-$. This reaction, which has a Q-value = -1.44 MeV, should provide a more accurate measure of the β^--energy spectrum than elastic scattering, because the kinetic energy of the β particle is essentially monoenergetic, 1.44-MeV less than that of the incoming ν_e. This charged-current (CC) interaction with the β^--particle occurs only for ν_e, not for the other neutrino flavors.

The neutral-current (NC) interaction, $^2D + \nu_x \rightarrow n + p + \nu_x$, can, on the other hand, be caused with equal probability by any of the three neutrino flavors, ν_x. The Q-value, -2.23 MeV, is simply the binding energy of the deuteron. This NC reaction is probably the most important one that SNO has the potential of detecting since the appearance of other neutrino flavors besides ν_e will be definitive proof of neutrino oscillations.

However, observation of the neutral-current signal depends upon the detection of the resulting neutrons, not an easy feat. Three different methods of neutron detection in D_2O (which acts as a neutron moderator) are being investigated in SNO; none of these will provide any directional or spectral information about ν_x:

(1) Neutron capture by the deuteron will produce ^3H + a prompt $\approx$6-MeV

γ-ray, which will produce Cerenkov light in the detector. However, this signal will have to be disentangled from the other sources of Cerenkov light; Monte Carlo simulations have been done to characterize these different signals.

(2) Addition of salt, NaCl, to the D_2O will enhance the neutron signal from the NC since neutron capture in ^{35}Cl produces a prompt $\approx$8-MeV γ-ray that gives rise to Cerenkov radiation. Taking the difference of the data obtained with the pure D_2O detector, and with the D_2O + NaCl, should accentuate the Cerenkov signal from neutron capture. However, this method is complicated by the fact that the NaCl must be removed from the 1000 tons of D_2O (by distillation), at least once, if not periodically. Another potential problem is due to the fact that the (n,γ) reaction on Na produces ^{24}Na. Its radioactive decay involves emission of γ rays with energies >2.23-MeV, which can cause photodisintegration of the deuteron, producing neutrons that can be mistakenly identified as coming from the NC interaction.

(3) Another method, which does not depend on production of Cerenkov light, is also being pursued. It is planned to count the neutrons directly with arrays of ^3He-filled proportional-counters suspended in the D_2O. This method requires the construction of leak-free counters from specially produced, ultra-pure materials so that no radioactive contamination is introduced into the D_2O.

We see that by virtue of its ability to detect both the CC and NC interactions of the neutrinos, SNO offers the possibility not only of verifying the deficit of ν_e but also of detecting for the first time the appearance of the other neutrino flavors, ν_x, that should result if neutrino oscillations do indeed occur.

However, even though great care is being taken to control the sources of radioactivity and other backgrounds in SNO (for example, an industrial clean room will be constructed in the mine at the detector site), its detection threshold will still be on the order of 5 MeV. Thus, like Super-Kamiokande, it will be sensitive only to the ^8B neutrino spectrum.

6.3. Borexino

The proposal to build Borexino [7] is based on using an organic liquid scintillator with high photon yield to detect neutrinos down to extremely low energies, $\geq$0.4 MeV. This value is 10× smaller than the 5-MeV detection threshold that is the characteristic goal of Super-Kamiokande and SNO. Borexino will be unique if it proves successful at making measurements at such low energies, and will be mainly sensitive to the solar ^7Be-neutrino branch.

The so-called "5-MeV (threshold) wall" that affects both Super-Kamiokande and SNO is primarily the result of decays of radioactive impurities, especially in the naturally occurring ^{238}U and ^{232}Th series, where energetic α particles and γ rays are emitted. In order to breach this wall and achieve the extremely low threshold that is its *sine qua non*, Borexino will have to attain impurity levels that are orders of magnitude lower than those of any other neutrino detector; *e.g.*, 10^{-16} g of uranium

or thorium and 10^{-14} g of potassium per g of detector. This is a formidable challenge.

In an early concept, the liquid scintillator would have contained a boron compound, trimethylborate, thus the name Borexino. The purpose of the boron in the scintillating medium was to measure the neutrino CC and NC reactions on the ^{11}B ground-state; CC would have produced excited states of ^{11}C, and NC, excited states of ^{11}B. The energy spectra of the γ rays emitted from these excited states would have then been measured by the liquid scintillator. However, the presence of boron in the scintillator introduces additional technical complications, and so it is not being actively pursued at the current time.

In the present version of Borexino, the energy of the recoil electrons resulting from neutrino elastic scattering will be measured by the liquid scintillator. The current plan is for Borexino to consist of $\approx$300 tons of liquid scintillator in a transparent spherical vessel, which is placed in an outer container that is filled with high purity H_2O. Phototubes mounted in the H_2O will view the scintillator. The fiducial region will consist of $\approx$100 tons of scintillator; the remaining scintillator and the outer H_2O will act as shielding. The plan is to construct Borexino at the Gran Sasso Laboratory (Italy).

However, because of the newness of its approach and the severe technical requirements of ultra-low impurity levels, Borexino is currently building an intermediate stage at Gran Sasso, known as the Counting Test Facility (CTF), to serve as a proof-of-principle facility. Although the CTF will not be a prototype of Borexino since it will not contain the large mass of shielding liquid outside of the sensititve central volume, it will serve to show if problems, anticipated or not, can be handled by the current design. The CTF will contain $\approx$4 tons of liquid scintillator, surrounded by H_2O. To prevent the buildup of radioactive contaminants in these liquids caused by leaching from the vessel walls, phototubes and other construction materials, or by deposition from the air, on-line chemical systems will periodically purify the organic scintillator and the water. Knowing and controlling the background levels in these liquids is extremely important; of almost equal importance are methods to measure and reduce the backgrounds in the construction materials of the inner and outer vessels, the backgrounds due to radon in the air and its nonvolatile daughters, and the external backgrounds.

The main goals of the CTF are to test the performance and reliability of the on-line purification systems, especially for the scintillator liquid, and to measure the concentrations of U, Th, K and ^{14}C at ultra-low levels. In some instances, analytical chemical methods cannot at present achieve the required sensitivity levels for some of these elements, so chemical research is needed. It may be that the ultimate determination of these impurities will not be attained until the CTF itself begins taking data.

Many of the components of the CTF are currently being built and tested. The plan is to begin operation in mid 1994. If no surprises are encountered and if CTF demonstrates that the required ultra-low background levels can be achieved and satisfactorily maintained, it is likely that permission will be given to begin

construction of the 300-ton Borexino detector. It is estimated that Borexino will begin operations some 2-years later, in the 1996-97 time frame.

7. ACKNOWLEDGMENTS

I am grateful to the following colleagues for providing me with up-to-date information and figures on the solar neutrino experiments in which they are involved: R. Davis for ^{37}Cl, A. Suzuki for Kamiokande, T. J. Bowles for SAGE, G. Ewan and A. McDonald for SNO, and R. Raghavan for Borexino.

8. REFERENCES

• Research sponsored by the U. S. Department of Energy, Office of High Energy and Nuclear Physics, under contract DEAC0276CH00016 with Brookhaven National Laboratory.

1. J. K. Rowley, B. T. Cleveland, R. Davis, *AIP Conf. Proc. No.126, Solar Neutrinos and Astronomy*, ed. M. L. Cherry, K. Lande, W. A. Fowler, p.1, AIP, New York, (1985).
2. K. S. Hirata *et al.*, *Phys. Rev. Lett.* **65**, 1297 (1990).
3. GALLEX Collaboration: P. Anselmann *et al.*, *Phys. Lett.* **B285**, 376 (1992).
4. A. I. Abazov *et al.*, *Phys. Rev. Lett.* **67**, 3332 (1991).
5. A. Suzuki, private communication.
6. G. Aardsma *et al.*, *Phys. Lett.* **B194**, 321 (1987); A. MacDonald and G. T. Ewan, private communication.
7. R. S. Raghavan *et al.*, in *Proc. 25th Intl. Conf. High Energy Phys.* ed. K. K. Phua, Y. Yamaguchi, p. 482, South Asia Phys. Soc. (1991); F. Calaprice, private communications.
8. K. Wolfsberg, private communication.
9. J. N. Bahcall, *Neutrino Astrophysics*, Cambridge University Press (1989).
10. J. N. Bahcall and M. H. Pinsonneault, *Rev. Mod. Phys.* **64**, 885 (1992).
11. J. N. Bahcall and R. Ulrich, *Rev. Mod. Phys.* **60**, 297 (1988).
12. S. Turck-Chieze, S. Cahen, M. Casse and C. Doom, *Astrophys. J.* **335**, 415 (1988).
13. S. Turck-Chieze and I. Lopes, *Astrophys. J.* **408**, 347 (1993).
14. R. Davis, in *Frontiers of Neutrino Astrophysics, Proc. Intl. Symp.*, ed. Y. Suzuki and K. Nakamura, p. 47, Universal Acad. Press, Tokyo (1993).
15. R. Davis, private communication.
16. K. S. Hirata *et al.*, *Phys. Rev. Lett.* **66**, 9 (1991).
17. GALLEX Collaboration: P. Anselmann *et al.*, *Phys. Lett.* **B285**, 390 (1992).
18. V. N. Gavrin *et al.*, *Proc. 26th Intl. Conf. High Energy Phys.* Dallas, in

press (1993); T. J. Bowles, private communications.
19. GALLEX Collaboration: P. Anselmann *et al.*, *Phys. Lett.* **B314**, 445 (1993).
20. S. P. Mikheyev, and A. Yu. Smirnov, *Sov. J. Nucl. Phys.* **42**, 1441 (1985); L. Wolfenstein, *Phys. Rev.* **D20**, 2634 (1979).
21. S. A. Bludman *et al.*, *Phys. Rev.* **D47**, 2220 (1993).
22. P. I. Kratsev and S. T. Petcov, *Phys. Lett.* **B285**, 85 (1992).